The American Journal of Pathology, Vol. 170, No. 5, May 2007

DOI: 10.2353/ajpath.2007.060703

Cell Injury, Repair, Aging and Apoptosis

Intrapulmonary Delivery of Ricin at High Dosage Triggers a Systemic Inflammatory Response and Glomerular Damage

John Wong,* Veselina Korcheva,*
David B. Jacoby,† and Bruce Magun*

From the Department of Cell and Developmental Biology and Division of Pulmonary and Critical Care Medicine,† Oregon Health and Science University, Portland, Oregon*

In view of the possibility that ricin may be used as a bioweapon against human populations, we examined the pathological consequences that occur in mice after introduction of ricin into the pulmonary system. Intratracheal instillation of a lethal dose of ricin (20 μg/100 g body weight) resulted in a hemorrhagic inflammatory response in multiple organs, accompanied by activation of mitogen-activated protein kinases, increased synthesis of proinflammatory RNA transcripts, and increased levels of circulating cytokines and chemokines. A sublethal dose of instilled ricin (2 μg/100 g body weight) induced a similar response in lungs but did not cause detectable damage in other organs. Lungs of mice that recovered from a sublethal dose of ricin displayed evidence of fibrosis and residual damage. A lethal dose of ricin caused accumulation of proinflammatory RNA transcripts and substantial damage to 28S rRNA of multiple organs, including lung, kidney, spleen, liver, and blood, demonstrating that instilled ricin gained access to the circulation. The kidneys of mice instilled with a lethal dose of ricin showed accumulation of fibrin/fibrinogen in glomerular capillaries, increased numbers of glomerular leukocytes, and impairment of kidney function. A sublethal dose of ricin failed to induce damage to 28S rRNA in kidney or other extrapulmonary organs. ***(Am J Pathol 2007, 170:1497–1510; DOI: 10.2353/ajpath.2007.060703)***

In view of ricin's high toxicity and ease of production, the United States Chemical Warfare Service began studying ricin as a weapon of war near the end of World War II.[1] The work performed in collaboration with the United Kingdom resulted in the development of a ricin-based bomb that was intended to disperse its payload by aerosolization. Although the weapon was tested, it was never used in battle. As a bioterrorist agent, ricin was first used in the assassination of Bulgarian defector Georgi Markov, whose body was penetrated by a 2-mm titanium ricin-containing pellet.[2] In recent years, ricin has become a tool of extremist groups in the United States and abroad.[3–6] Because of its potential use as a terrorist weapon and its ease of delivery to large populations by aerosolization, ricin meets the criteria for an agent of warfare[2] and is currently listed as a category B priority pathogen for study in the biodefense strategic plan presented by the United States National Institute of Allergy and Infectious Diseases.

Ricin is a 62-kd protein consisting of a 34-kd B chain that binds primarily to galactose-containing surface proteins, which facilitate internalization of the toxic 32-kd A chain through receptor-mediated endocytosis.[7] The A chain then enters the cytosol, where it depurinates a single adenine in the sarcin/ricin loop of 28S rRNA.[8] The depurination of this critical adenine (A4256 in mice) prevents the binding of elongation factor-2, thereby blocking protein translation.[9] Depurination of A4356 simultaneously activates a kinase cascade that leads to the phosphorylation and activation of the stress-activated protein kinases (SAPKs), c-Jun-N-terminal kinase (JNK), and p38 mitogen-activated protein (MAP) kinase (MAPK),[10] which belong to the MAPK kinase superfamily and have been tied to the transcriptional and posttranscriptional activation of proinflammatory genes.[11,12] Blockade of SAPKs in cultured cells by small molecule inhibitors leads to substantial suppression of ricin-induced proinflammatory mRNA transcripts.[13]

Supported by the National Institutes of Health (grants ES889456 and AI1059335).

Accepted for publication January 26, 2007.

Supplementary material for this article can be found on *http://ajp.amjpathol.org*.

Address reprint requests to Bruce Magun, Oregon Health and Science University, 3181 SW Sam Jackson Park Rd., Portland, OR 97239. E-mail: magunb@ohsu.edu.

Ricin belongs to a group of ribosome-inactivating proteins, also known as ribotoxins, which have a similar structure and mechanism of action.[14] Shiga toxins are ribotoxins produced by *Escherichia coli* serotype O157:H7 and are responsible for the development of hemolytic uremic syndrome, which is characterized by hemolytic anemia, thrombocytopenia, and acute renal failure.[15] Previously, we and others have reported that intravenous administration of ricin to mice recapitulates many of the symptoms of hemolytic uremic syndrome, including thrombotic microangiopathy, hemolytic anemia, thrombocytopenia, increases in plasma-borne cytokines, and acute renal failure.[13,16,17] Analysis of proinflammatory gene expression in multiple organs revealed that intravenous ricin induced a robust response, coincident with the symptoms of hemolytic uremic syndrome.

In view of the potential dissemination of ricin to human populations by aerosolization, it is critical to understand the pathological consequences of ricin poisoning in the lungs and possibly other tissues. Aerosol delivery of ricin to animals results in a severe inflammatory response characterized by increased inflammatory cell counts[18] and apoptosis of alveolar macrophages.[19] After aerosol exposure, the pathology is essentially restricted to the lungs.[20] Previous studies using inhaled ^{125}I-ricin in mice revealed that only a small fraction of the radioactivity reaching the lungs was transferred to extrapulmonary sites.[21] In these experiments, the authors conjectured that the ^{125}I-ricin was degraded within the lung and that most of the radioactivity that appeared in the circulation was probably in the form of free ^{125}I.

In the present study, we have instilled lethal and sublethal doses of ricin into the tracheae of mice and have examined a number of responses in pulmonary and extrapulmonary tissues including activation of MAP kinase family members, elevation of transcripts that encode inflammatory proteins, the presence of circulating inflammatory cytokines, and apoptotic responses. We provide evidence that a lethal dose of instilled ricin caused a severe hemorrhagic inflammatory response in pulmonary tissues, entered the vascular system, and initiated inflammatory responses in multiple organ sites. Especially notable were the responses seen in kidneys, which exhibit accumulation of fibrin/fibrinogen in glomerular capillaries, increased numbers of glomerular leukocytes, and impaired kidney function. By contrast, a lower, nonlethal, dose of instilled ricin induced primarily a localized inflammatory response in lungs with detectable, but minimal, evidence of systemic effects. The sublethal dose of ricin failed to cause hemorrhage within pulmonary tissues. After resolution of inflammation, animals receiving lower doses of ricin displayed areas of fibrosis and destruction of airway tissue.

Materials and Methods

Mice

All studies were conducted with approval by the Institutional Animal Care and Use Committee at Oregon Health and Science University. Male C57BL/6 mice (5 to 8 weeks old) from The Jackson Laboratory (Bar Harbor, ME) were used and were kept in microisolator cages. For instillation, mice were anesthetized with an intraperitoneal injection of 2 mg of ketamine and 0.2 mg of xylazine. A 20-gauge catheter (Exel, Culver City, CA) was then inserted into the opening of the trachea with the aid of a pediatric otoscope. After attaching the catheter to a syringe, 50 μl of saline or the same volume of ricin (Vector Laboratories, Burlingame, CA) was delivered at indicated concentrations.

Antibodies

Antibody against Gr-1 (no. 550291) was purchased from BD Bioscience Pharmingen (San Jose, CA). Antibodies against phospho-extracellular signal-regulated kinase (ERK) (no. 9101), phospho-JNK (no. 9251), phospho-p38 (no. 4631), and active caspase 3 (nos. 9661 and 9664) were purchased from Cell Signaling Technology (Danvers, MA). Antibody against fibrin/fibrinogen (no. YNGMFbg7S) was purchased from Accurate Chemical and Scientific (Westbury, NY). Antibodies against p38 (no. sc-535) and the p65 subunit of nuclear factor (NF)-κB (no. sc-372-G) were purchased from Santa Cruz Biotechnology (Santa Cruz, CA).

Histology and Immunohistochemistry

Animals were sacrificed at 48 hours unless indicated otherwise. After anesthesia, mice were perfused with 4% paraformaldehyde, and tissues were removed and fixed overnight in the same fixative. For staining of fibrin/fibrinogen, unperfused tissues were harvested, fixed in Carnoy's fixative for 2 hours, and stored in 70% ethanol. All tissues were dehydrated and embedded in paraffin. For histology, 5-μm sections were mounted on glass slides, deparaffinized, and stained with hematoxylin and eosin (H&E) following standard procedures. For immunohistochemical analysis of most antigens, antigen retrieval was performed by placing the deparaffinized slides in 10 mmol/L sodium citrate (pH 6) in a microwave oven for 10 minutes. Immunohistochemical demonstration of Gr-1 and fibrin/fibrinogen did not require pretreatment for antigen retrieval. After blocking in serum, the slides were incubated with primary antibodies overnight at 4°C at appropriate dilutions. Slides were further processed using the VectaStain Elite ABC kit (Vector Laboratories) according to the manufacturer's recommendations using 3,3′-diaminobenzidine as substrate. Immunohistochemical analysis was performed on specimens from at least three saline-treated animals and three ricin-treated animals to verify reproducibility.

Immunoblotting

Tissues were snap-frozen in liquid nitrogen and disrupted in lysis buffer as previously described.[13] Equal amounts of protein of each lysate were separated on a 10% denaturing polyacrylamide gel in the presence of sodium

dodecyl sulfate-polyacrylamide gel electrophoresis (SDS-PAGE) and transferred onto polyvinylidene difluoride membranes according to standard laboratory procedures. Membranes were incubated with the indicated antibodies and the corresponding horseradish peroxidase-conjugated secondary antibodies; signals were detected using enhanced chemiluminescence.

Microarray Analysis

Gene expression profiling was performed by the Gene Microarray Shared Resource Affymetrix Microarray Core at Oregon Health and Science University. To verify RNA integrity, total RNA was run on 1% agarose gels. Pooled samples from three saline-treated mice and three ricin-treated mice were analyzed on a bioanalyzer (Agilent, Palo Alto, CA). After reverse transcription, each of the two labeled target cDNA pools was hybridized to the GeneChip Mouse Genome 430 2.0 array (Affymetrix, Santa Clara, CA), which interrogates 39,000 transcripts. Data were processed using the Affymetrix Microarray Suite 5.0 (MAS 5.0) software and further analyzed using the EASE software distributed by the National Institutes of Health (*http://david.abcc.ncifcrf.gov/home.jsp*).

Real-Time Reverse Transcriptase-Polymerase Chain Reaction (RT-PCR)

Tissues were harvested, snap-frozen in liquid nitrogen, and stored at −70°C. Total RNA from frozen tissues and fresh blood was isolated using TRIzol (Invitrogen, Carlsbad, CA) following the manufacturer's instructions. RNA was treated with DNase I (Invitrogen) and reverse-transcribed with SuperScript II and oligo dT primer (Invitrogen). Real-time PCR was performed using SYBR Green reagents on an ABI Prism 7900HT (Applied Biosystems, Foster City, CA); fold induction was calculated with the absolute quantification method using levels of glyceraldehyde phosphate dehydrogenase (GAPDH) for normalization. The nucleotide sequences of the primers used in this study have been previously published.[13]

Multiplex Cytokine Detection

Levels of secreted chemokines and cytokines from three saline-treated and three ricin-treated mice were analyzed using a customized Multiplex mouse cytokine kit from Linco Research (St. Charles, MO) and detected on the LiquiChip Workstation (Qiagen, Valencia, CA).

Primer Extension for Visualizing Lesions in 28S rRNA

Reverse transcription of rRNA with a ^{32}P-radiolabeled primer has previously been described.[10] Reverse-transcribed reaction products from total RNA from a variety of tissues were resolved by electrophoresis in 8% acrylamide gels containing 50% urea. Signals were detected on a PhosphorImager (Molecular Dynamics/Amersham, Piscataway, NJ). Quantification of percent 28S rRNA containing ricin-specific lesions was performed as described.[13]

Protein Analysis in Urine

Urine was collected from mice housed in diuresis metabolic cages and concentrated by ultrafiltration. Equal amounts of urine from three control mice and three ricin-treated animals were loaded and separated by SDS-PAGE. Various concentrations of bovine serum albumin were loaded on the same gel to mark the position of serum albumin. Gels were stained with Gelcode Blue solution (Pierce, Rockford, IL).

Blood Urea Nitrogen Determination

Measurement of blood urea nitrogen in serum from three saline-treated mice and three ricin-treated mice was performed with a Synchron LX clinical chemistry system (Diagnostic Chemicals, Oxford, CT).

Statistical Analysis

Individual groups were compared using unpaired *t*-test analysis. To determine *P* values, all statistical analyses were interpreted in a two-tailed manner. *P* values <0.05 were considered to be statistically significant.

Results

To determine the consequences of ricin-induced lung injury in a mouse model, we delivered a range of ricin doses to groups of mice by intratracheal instillation. Our goal was to identify a dose of ricin that would produce acute lethal injury and a nonlethal dose with residual effects that could be analyzed after recovery of the animals. The LD_{50} for instilled ricin was ~10 μg of ricin/100 g body weight. All mice receiving 20 μg of ricin/100 g body weight displayed weight loss and developed labored breathing and ataxia at 48 hours. These animals were unresponsive to external stimuli and were judged to be moribund. In accordance with Institutional Animal Care and Use Committee guidelines, these mice were euthanized at that time, and their tissues were processed for pathological analysis. Animals receiving 2 to 5 μg of ricin/100 g body weight showed similar but diminished symptoms, remained responsive to stimuli, and eventually recovered.

Responses to a Lethal Dose of Ricin

To determine the pathological features of acute, lethal, lung injury, we instilled 20 μg of ricin/100 g body weight into mice, and sacrificed animals for histological analysis of lungs at various times up to 48 hours. Histopathological changes, observed not earlier than 48 hours after instillation of ricin, included perivascular and peribronchial edema accompanied by denudation and/or disrup-

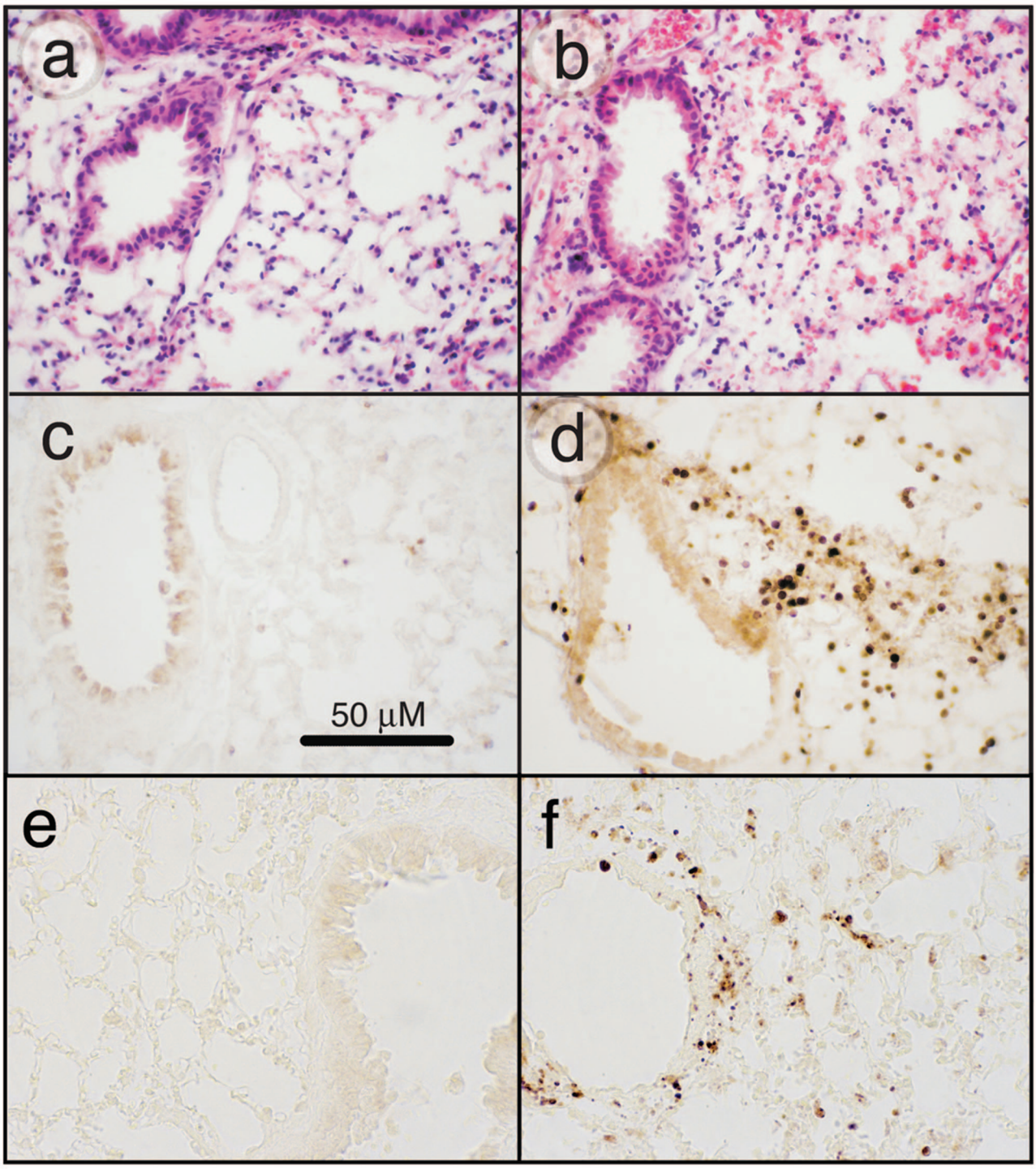

Figure 1. Effects of ricin on lung tissues. C57BL/6 mice were instilled intratracheally with 50 μl of saline (**a**, **c**, **e**) or 20 μg of ricin/100 g body weight (**b**, **d**, **f**), and tissues were harvested at 48 hours. **a** and **b:** H&E-stained tissue sections. Tissue from ricin-instilled lung (**b**) showed perforations in the bronchiolar epithelium, evidence of hemorrhage, and influx of leukocytes. **c** and **d:** Immunohistochemical detection of Gr-1. Tissue from ricin-instilled lung showed accumulation of Gr-1-positive cells in peribronchiolar (**d**) and perivascular locations (not shown). Counterstaining of nuclei with methyl green (not shown) confirmed that the Gr-1-positive cells were neutrophils. **e** and **f:** Immunohistochemical detection of activated caspase 3. Original magnifications, ×400.

tion of the bronchial epithelium (Figure 1, a and b). All tissue sections revealed extensive pathology, although regions of apparently normal histology were also observed among these areas. In some regions, extravasated erythrocytes were plentiful, indicative of hemorrhage. Neutrophils were abundant in perivascular and peribronchial/periobronchiolar regions, as demonstrated by immunohistochemical detection of the Gr-1 epitope (Figure 1, c and d). Some parenchymal areas contained alveolar exudate and intra-alveolar neutrophils. Disruption of the bronchial epithelium was frequently associated with apoptotic bodies, indicating the presence of apopto-

tic cells in these regions. Evidence of apoptotic cells in bronchial epithelium and within the interstitium is shown in Figure 1, e and f. These results demonstrated that instillation of ricin induced a robust inflammatory response accompanied by cell death and suggested that the entrance of ricin into interstitial regions of the pulmonary parenchyma may have been facilitated by disruption of the bronchial epithelium.

The binding of leukocytes to endothelial selectins during inflammation generates signals that result in the deposition of fibrin and the initiation of thrombosis.[22] To determine whether deposition of fibrin occurred after the administration of ricin, we used an antibody specific for the immunohistochemical detection of fibrin/fibrinogen. Fibrin/fibrinogen was deposited abundantly throughout the lungs of mice that had received 20 μg of ricin/100 g body weight for 48 hours but was absent from the lungs of control mice (Figure 2, a and b). Examination of tissue sections at higher magnification revealed that the reaction product was localized primarily within the microvasculature of the alveolar septa (Figure 2c, arrows).

Previous studies demonstrated that the elevation of proinflammatory transcripts by intravenously administered ricin results from the activation of the MAPK family members ERK, JNK, and p38 MAPK.[13] To determine whether instilled ricin would activate these kinases, we subjected lung tissue lysates to analysis by immunoblotting 48 hours after intratracheal instillation of 20 μg of ricin/100 g body weight (Figure 3a). Instillation of ricin led to increased phosphorylation of ERK and JNK, but not p38 MAPK (Figure 3, lanes 1 to 3 versus lanes 5 to 8), probably attributable to the substantially activated state of the latter kinase in the lungs of control mice. Activation of ERK and JNK by ricin was confirmed by immunohistochemical analysis by using antibodies specific for the phosphorylated forms of these MAPKs (Figure 3, b–e). The reaction product was localized to bronchial/bronchiolar epithelial cells, alveolar epithelial cells, and endothelial cells and was primarily intranuclear. Immunohistochemical reactivity of phosphorylated p38 MAPK was similar in control and ricin-instilled lungs (Figure 3, f and g), consistent with the results obtained by immunoblotting (Figure 1a). Examination of tissues by immunohistochemistry at earlier times (6 to 24 hours) demonstrated that the phosphorylation of ERK and JNK induced by ricin was evident at 6 hours and that the intensity of the reaction product increased thereafter (not shown).

In the respiratory system, increased NF-κB activity contributes to the pathogenesis of acute respiratory disease syndrome and inflammatory disease.[23] On activation, NF-κB migrates from cytoplasm to nucleus, where it fulfills its function as a transcription factor. To detect the possible ricin-mediated activation of NF-κB by immunohistochemistry, we applied an antibody directed against its p65 subunit (RelA; Figure 3, h and i). Intense reactivity of NF-κB was seen in the nuclei of most cell types in lungs of ricin-instilled animals 48 hours after instillation (Figure 3i) but not in lungs from control animals (Figure 3h).

The immunohistochemical detection of activated caspase 3, a reliable apoptotic marker, revealed the presence of apoptotic cells in lungs of ricin-instilled mice but not in lungs of control mice 48 hours after instillation of ricin (Figure 1, e and f). The reaction product in lungs from ricin-treated animals was localized to patches of airway cells and to scattered cells within the alveolar parenchyma. Localization of apoptotic cells was verified using three different antibodies against the p17/p19 subunit of caspase 3; in addition, we detected the appearance of this cleaved product by immunoblotting (data not

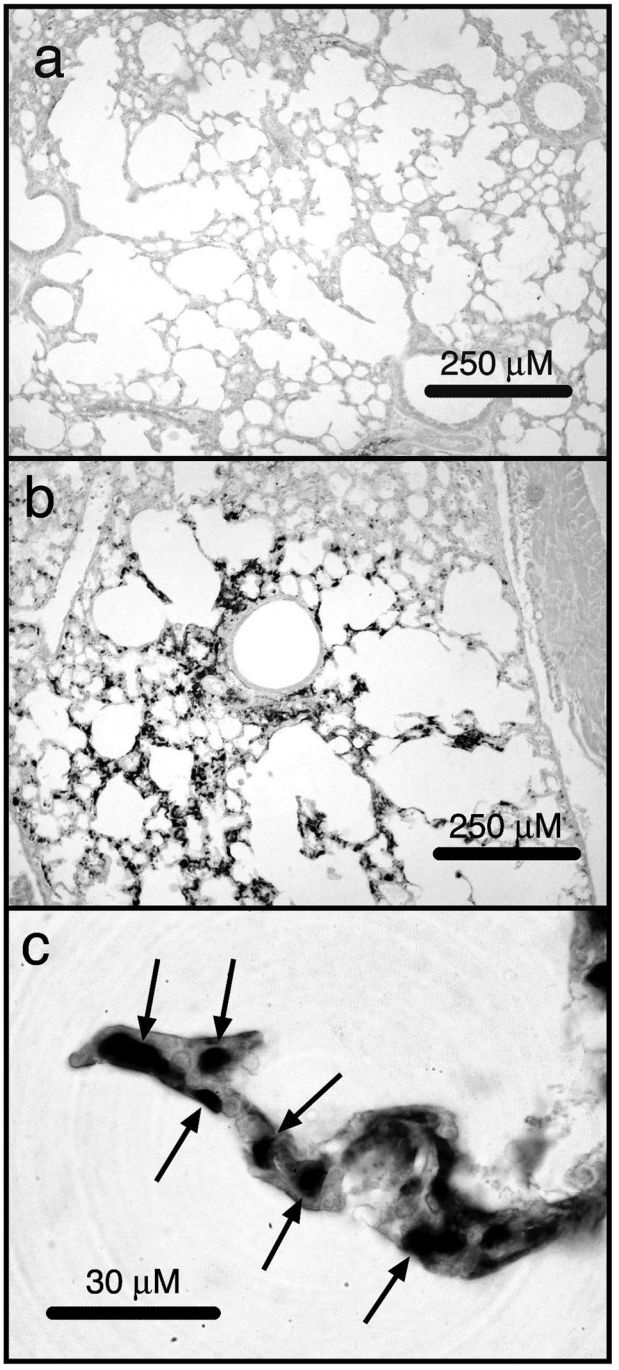

Figure 2. Accumulation of fibrin/fibrinogen in lung tissues. Mice were instilled with saline (**a**) or 20 μg of ricin/100 g body weight (**b**) before the harvesting of tissues 48 hours later. Tissue sections were incubated with an antibody specific for fibrin/fibrinogen. **c:** Increased deposition of reaction product within the microvasculature of an alveolar septum. Original magnifications: ×100 (**a**, **b**); ×1000 (**c**).

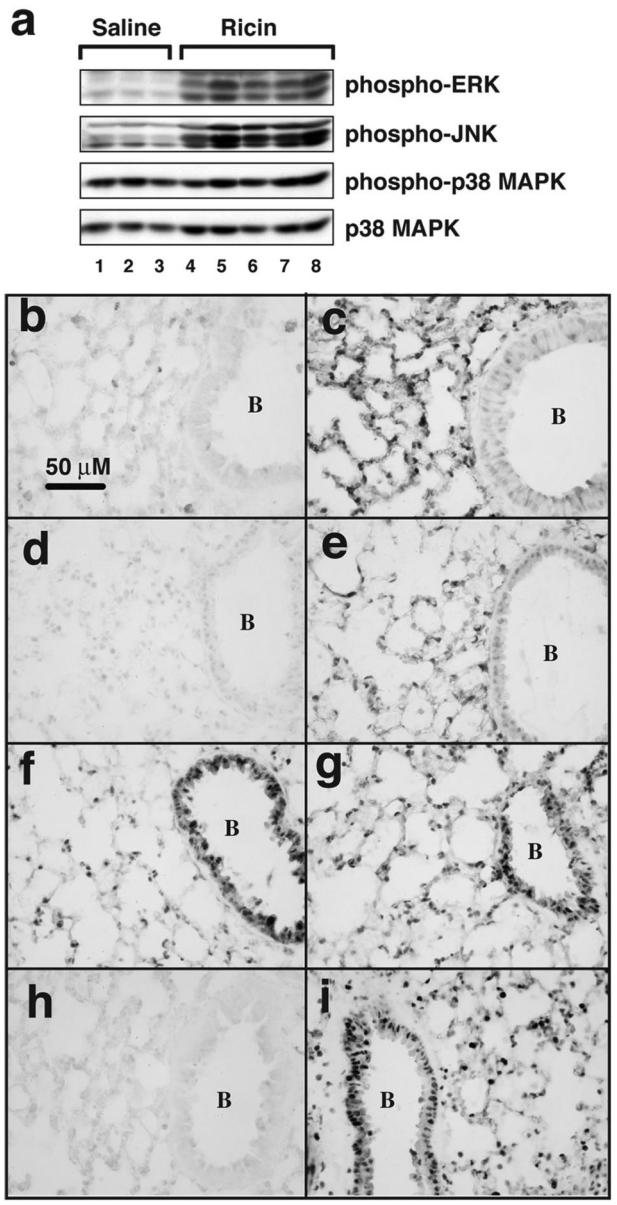

Figure 3. Activation of signaling pathways in lung tissues. **a:** Protein lysates from three mice instilled with saline and five mice instilled with 20 μg of ricin/100 g body weight were harvested 48 hours later and subjected to immunoblotting using antibodies against the phosphorylated forms of ERK, JNK, and p38 MAPK and against the nonphosphorylated form of p38 MAPK (as loading control). Tissues from mice instilled with saline (**b**, **d**, **f**, **h**) or ricin (**c**, **e**, **g**, **i**) were subjected to immunohistochemical staining using antibodies against phospho-ERK (**b**, **c**), phospho-JNK (**d**, **e**), phospho-p38 (**f**, **g**), and the p65 subunit of NF-κB (**h**, **i**). B denotes the interior of a bronchiole. Original magnifications, ×400.

shown). A similar analysis was performed on spleen, kidney, and liver from the same animals examined in Figure 3. Immunoblotting did not reveal an increased phosphorylation of ERK, JNK, or p38 MAPK in these tissues (data not shown). However, immunohistochemical detection revealed a slight increase in nuclear accumulation of these phosphorylated proteins (data not shown).

Taken together, the data in Figures 1 to 3 demonstrate that the intratracheal administration of a lethal dose of ricin resulted in severe injury and inflammation of the airways and alveoli, characterized by influx of neutrophils, focal areas of hemorrhage, necrosis, and apoptosis of the airway epithelium and cells of the alveolar parenchyma. The robust activation of ERK, JNK, and NF-κB was consistent with the well-characterized participation of these signaling pathways in the development and maintenance of an intense inflammatory response.

The intranuclear phosphorylation of transcription factors by activated MAPK members and the nuclear migration of activated NF-κB are predominant mechanisms by which proinflammatory signals lead to the transcriptional activation of proinflammatory genes.[24,25] To determine the identities of transcripts that increase in response to a lethal dose of ricin, we performed microarray analysis on RNA from sham- and ricin-instilled lungs 48 hours after instillation. The analysis was performed on Affymetrix MOE-430 2.0 microchips, which interrogate ~39,000 mouse transcripts. Of the 14,000 annotated genes interrogated, the administration of ricin caused the up-regulation of 400 genes in 10-fold excess (false discovery rate-adjusted P value <0.01; Supplementary Table 1, see *http://ajp.amjpathol.org*). A large number of up-regulated transcripts were encoded by genes that are known to be associated with organ injury and inflammatory responses, including chemokines, cytokines, transcription factors, leukocyte adhesion molecules, and acute phase proteins. The data obtained from the microarray analysis of genes with transcripts up-regulated more than 10-fold by ricin were analyzed by EASE, a software application for the rapid interpretation of biological data from microarray analysis.[26] The EASE software automates the process of biological theme determination for sets of selected, annotated, genes and provides a confidence value (P value) for genes associated with specific molecular processes and biological functions. As verified by EASE analysis (Table 1), the biological processes associated with the transcripts that were increased in abundance greater than 10-fold were related to injury, response to stress, innate immunity, and inflammatory responses. The molecular functions assigned to genes that were overrepresented in the EASE analysis included cytokines, chemokines, growth factors, and receptors.

Verification of results from microarray analysis was performed by quantitative real-time RT-PCR analysis of independent RNA samples obtained from a subsequent experiment in which groups of three mice were instilled either with 20 μg of ricin/100 g body weight or with saline as control. For analysis, we selected a set of genes that has been shown to be associated with inflammatory phenomena: cytokines [tumor necrosis factor (TNF)-α, interleukin (IL)-1β, and IL-6], chemokines (CXCL1 and CCL2), transcription factors (c-Fos, c-Jun, and EGR-1), and an adhesion molecule (E-selectin). The results, expressed as fold induction (using GAPDH as an invariant comparator), verified the ricin-mediated increases in the selected RNAs in lungs (Figure 4, open bars). In most cases, the ricin-mediated fold increase determined by quantitative real-time RT-PCR exceeded the value obtained by Affymetrix microarray analysis (Supplementary Table 1, see *http://ajp.amjpathol.org*), consistent with the limited

Table 1. Overrepresentation Analysis of Annotated Ricin-Induced Gene Expression in Lung

Gene ontogeny group	Hits	Total in category	*P* value (EASE score)
Biological process			
Defense response	34	429	4.05e-15
Response to pathogen	24	194	1.24e-14
Immune response	30	343	2.31e-14
Innate immune response	16	193	8.01e-12
Inflammatory response	15	90	6.92e-11
Response to wounding	18	162	3.45e-10
Response to stress	28	450	6.46e-10
Response to chemical substance	13	115	1.72e-07
Chemotaxis	11	76	2.15e-07
Cell motility	13	154	4.02e-06
Molecular function			
Cytokine activity	21	167	2.11e-13
Chemokine activity	11	35	3.79e-11
G-protein receptor binding	11	37	7.02e-11
Receptor binding	25	371	4.44e-10
Growth factor activity	12	121	1.25e-06

dynamic range that is associated with microarray technology.

The abundant increase in expression of mRNA encoding proinflammatory cytokines in the lungs of ricin-instilled mice suggests that some mediators may enter the circulation to cause widespread systemic inflammatory effects. To test this validity of this hypothesis, we obtained sera from ricin-instilled and sham-instilled mice 48 hours after instillation of 20 μg of ricin/100 g body weight and measured the concentration of several cytokines and chemokines in the serum of each mouse. Mice receiving instilled ricin revealed significant ($P < 0.05$) increases in several circulating cytokines (TNF-α, IL-1β, and IL-6) and chemokines (CXCL1 and CCL2; Figure 5).

The increased levels of circulating cytokines in mice instilled with a lethal dose of ricin suggested that the

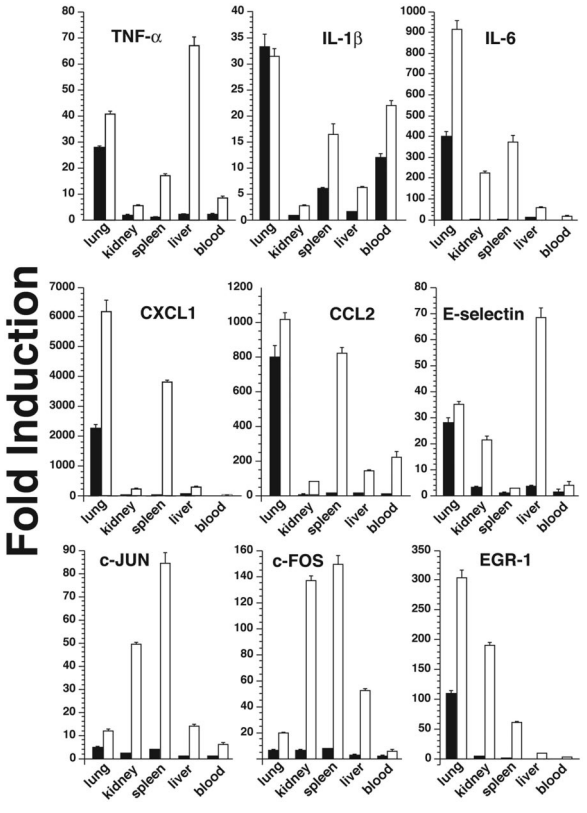

Figure 4. Increased expression of proinflammatory transcripts in multiple organs. Total RNA was purified from lung, kidney, liver, spleen, and blood of three mice treated with either saline or 20 μg of ricin/100 g body weight. Real-time RT-PCR was then performed on RNA extracted from organs of each mouse using primers specific for the indicated gene products. The data obtained by real-time RT-PCR on RNA from lung in this experiment is presented in Table 1. Absolute quantitation was first calculated in arbitrary units using standard curves and then normalized against GAPDH levels. Fold induction for each organ was then determined to show changes in expression induced by ricin.

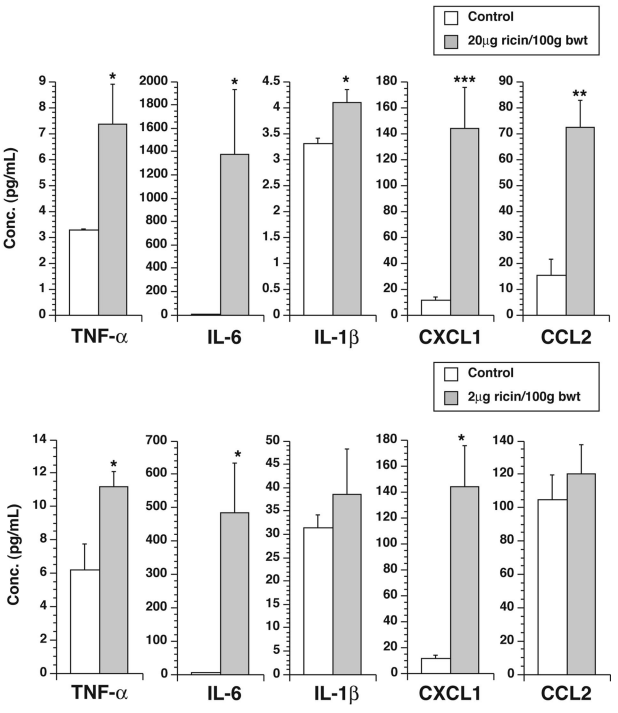

Figure 5. Increased levels of cytokines and chemokines in sera of mice instilled with ricin. Sera were collected from groups of three mice instilled with saline (open bars), 20 μg of ricin/100 g body weight (filled bars, top), or 2 μg of ricin/100 g body weight (filled bars, bottom), 48 hours after instillation. Cytokines and chemokines were measured as described in Materials and Methods. $^{*}P < 0.05$; $^{**}P < 0.01$; $^{***}P < 0.001$.

delivery of ricin to the lungs may activate inflammatory responses in other organ sites. To determine whether mice that received a lethal dose of intratracheal ricin would respond by expressing RNA transcripts encoded by proinflammatory genes in extrapulmonary tissues, we harvested RNA from kidney, liver, spleen, and blood to determine the level of expression of transcripts by real-time RT-PCR (Figure 4, open bars). Although the expression of proinflammatory transcripts in ricin-instilled mice was most frequently higher in lung than in other organs, most transcripts examined in extrapulmonary tissues were elevated significantly over sham-instilled controls.

The ability of ricin to elevate the expression of proinflammatory RNA transcripts in extrapulmonary tissues may be caused by the systemic action of lung-derived cytokines, such as TNF-α, and/or more directly by the action of circulating ricin. The ability of ricin to depurinate A^{4256} in 28S rRNA was used as a highly sensitive and specific test for the direct action of ricin in tissues. Accordingly, we extracted RNA from several organs after instillation of ricin and in each sample determined the fraction that harbored lesions at A^{4256} in the peptidyl transferase ring of 28S rRNA. The assay used is based on reverse transcriptase-mediated extension of cDNA from a ^{32}P-labeled primer that has been annealed to 28S rRNA downstream from the target site within the peptidyl transferase ring.[10] The cDNA generated from lesioned 28S rRNA molecules is shorter than cDNA generated from intact 28S rRNA because the reverse transcriptase is unable to proceed across the depurinated nucleic acid residue. Radiolabeled cDNA derived from intact and lesioned RNA can thus be distinguished from each other by polyacrylamide gel electrophoresis on the basis of size, and the proportion of affected 28S rRNA can be accurately measured.[10]

The cDNA transcribed from 28S rRNA derived from lung, blood, kidney, liver, and spleen of ricin-instilled animals displayed a prominent radioactive transcript truncated at A^{4256}, whereas the cDNA transcribed from brain RNA lacked a corresponding band (Figure 6a). Quantitative analysis revealed that 26% of the transcripts from both lung and kidney were truncated at A^{4256}. By comparison, the percentage of transcripts truncated at A^{4256} from blood, liver, and spleen RNA was lower (13, 6, and 16%, respectively). RNA extracted from brain tissue did not reveal damage to 28S rRNA. These results demonstrate that the intratracheal delivery of 20 μg of ricin/100 g body weight resulted in the distribution of ricin to many remote organ sites, where it was able to interact directly with 28S rRNA of target cells.

When ricin is administered intravascularly to mice, the kidneys exhibit profound pathological responses, including vascular stasis, deposition of fibrin in glomeruli, proteinuria, and other changes symptomatic of renal failure.[13] The appearance of comparable numbers of lesions in 28S rRNA in lung and kidneys of ricin-instilled mice (Figure 6a) suggested that the kidney may serve as a relevant target of ricin under the experimental conditions that were applied. Histopathological examination of kidney sections after H&E staining revealed mild accumulation of inflammatory cells of mixed origin into the

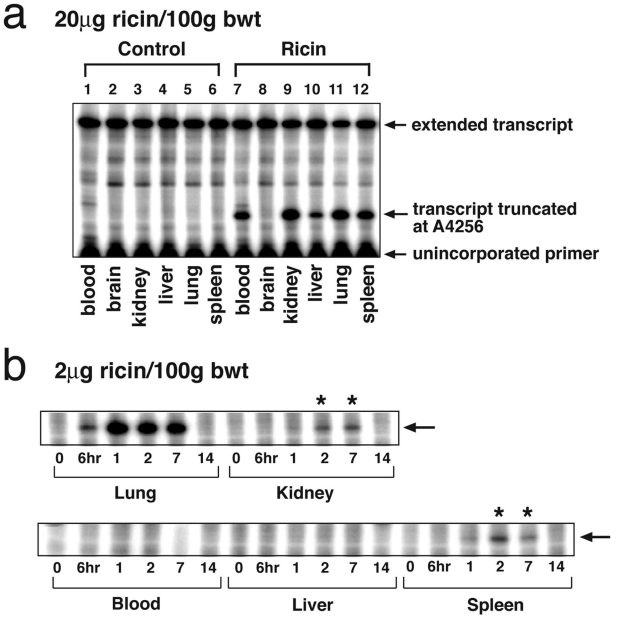

Figure 6. Primer extension showing lesions in 28S rRNA in multiple tissues. **a:** Total RNA was purified from blood, brain, kidney, lung, liver, and spleen of mice instilled with saline (**lanes 1** to **6**) or 20 μg of ricin/100 g body weight (**lanes 7** to **12**) and sacrificed 48 hours after instillation. Reverse transcription was performed using a primer that binds near the known ricin-mediated depurination site of the 28S rRNA[10,13] to detect the presence of stalled transcripts. Truncated transcripts were detected from all ricin-treated tissues except brain. **b:** Mice were instilled with 2 μg of ricin/100 g body weight and blood, kidney, lung, liver, and spleen were harvested at times from 6 hours to 14 days, as indicated. Total RNA was purified and primer extension was performed as described above.

glomerular capillary loops of mice instilled intratracheally with 20 μg of ricin/100 g body weight 48 hours before sacrifice (not shown). Quantitative assessment of glomerular neutrophilia was performed by immunohistochemical staining of tissues with an antibody specific for Gr-1, a reliable marker for neutrophils.[27] Glomeruli from ricin-instilled mice revealed a sevenfold increase in numbers of neutrophils, compared with saline-instilled control mice (Figure 7a). Immunohistochemical staining of kidney tissue with an antibody specific for fibrin/fibrinogen revealed substantial deposition of reaction product within glomerular and interstitial capillaries of ricin-instilled mice, but not in saline-instilled control mice (Figure 7, b and c). To determine whether kidney function was compromised in ricin-instilled mice, urine was collected from mice and examined for content of serum albumin. Electrophoresis of urine from ricin-instilled mice revealed a prominent band of protein corresponding in size to serum albumin, which was absent in urine from control mice (Figure 8). Further evidence of impaired kidney function was demonstrated by an increase in blood urea nitrogen from 20.7 $\pm$ 1.6 mg/dl in control animals to 51.0 $\pm$ 10.8 mg/dl in ricin-instilled animals ($P < 0.05$). Taken together, these studies demonstrate that a lethal dose of ricin delivered by intratracheal instillation achieved distribution to multiple organs, produced systemic inflammatory responses, and resulted in glomerular pathology associated with compromised kidney function.

To examine the possibility that the entry of ricin into the systemic circulation could have occurred via the gastro-

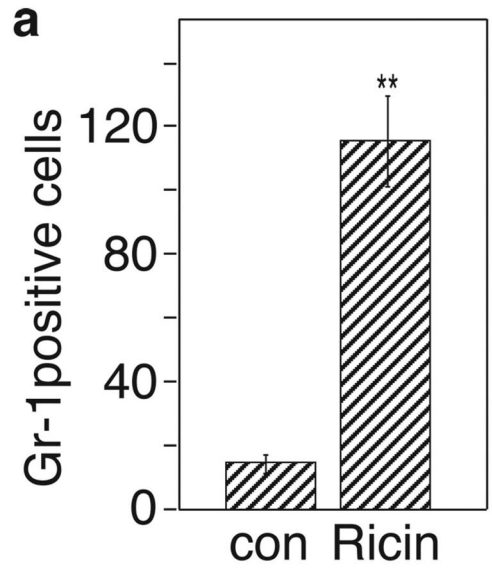

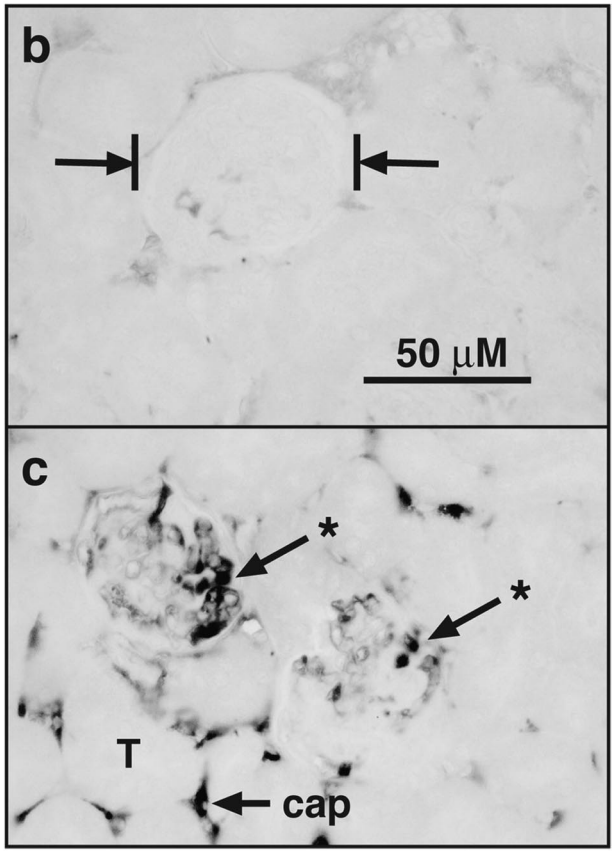

Figure 7. Increased accumulation of Gr-1-positive cells and fibrin/fibrinogen in glomeruli of ricin-instilled mice. Groups of three mice were instilled with saline or 20 μg of ricin/100 g body weight and sacrificed 48 hours later. **a:** Kidneys were harvested and examined by immunohistochemistry with an antibody specific for Gr-1. Gr-1-positive cells found in glomeruli in an entire sagittal kidney section from each animal were counted. $^{**}P < 0.01$. **b:** Tissue sections were examined by immunohistochemistry with an antibody specific for fibrin/fibrinogen. **b:** Vertical bars indicate the location of a representative glomerulus from kidney of a saline-instilled mouse. **c:** Reaction product (*) is deposited within glomerular and interstitial capillaries of ricin-treated tissues; T shows the location of a tubule, and cap indicates an interstitial capillary. Original magnifications, ×400 (**b** and **c**).

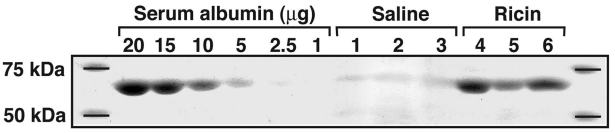

Figure 8. Albuminuria after instillation of ricin. Animals were treated with saline or 20 μg of ricin/100 g body weight. Urine samples were collected throughout 48 hours in metabolic cages. Equal amounts of urine from three saline- or ricin-instilled mice were concentrated and examined by SDS-PAGE as indicated (**lanes 1** to **6**). Varying concentrations of bovine serum albumin, as indicated, were loaded onto the gel to serve as indicators.

intestinal tract (eg, by ingestion of toxin or by inadvertent experimental delivery), we intentionally instilled 20 μg of ricin/100 g body weight into the esophagus. Co-instillation of a tracer dye verified that the solution had entered the gastrointestinal tract. Animals treated in this manner did not respond by increased expression of proinflammatory transcripts in blood, lungs, kidneys, liver, or spleen, nor did the RNA extracted from these organs reveal lesions in 28S rRNA (data not shown). These experiments demonstrated that entrance of ricin into the circulation, at the dose of ricin applied, would not have occurred through a gastrointestinal route.

Responses to a Sublethal Dose of Ricin

It would be important to understand both acute and residual effects induced by ricin after exposure of human populations. Exposure of mice to graded doses of ricin revealed that an intratracheal dose of 2 μg of ricin/100 g body weight or less did not cause mortality. Although animals exposed to this dose initially lost weight and exhibited some ataxia, the animals eventually recovered and survived. Similar to the effects of a lethal dose of ricin (Figure 1, c and d), 48 hours after administration of a sublethal dose of ricin lungs showed focal parenchymal accumulation of inflammatory infiltrate containing predominantly neutrophils (Figure 9, compare a and b to c and d). As in animals exposed to a lethal dose of ricin (Figure 3), lungs from animals receiving 2 μg of ricin/100 g body weight demonstrated increased phosphorylation of ERK and JNK at 48 hours as revealed by both immunoblotting and histochemistry and demonstrated increased expression of nuclear NF-κB by immunohistochemistry (not shown). Animals instilled with 2 μg of ricin/100 g body weight also displayed extensive apoptosis, as revealed by immunoblotting (cleavage of caspase 3) and immunohistochemical reactivity of cleaved caspase 3. However, in contrast to animals subjected to a lethal dose of ricin, animals receiving a sublethal dose of ricin failed to display evidence of hemorrhage or deposition of fibrin in pulmonary tissues. When examined 4 weeks after administration of 2 μg of ricin/100 g body weight, lungs did not show evidence of residual leukocytosis (data not shown). However, at that time animals showed moderate interstitial deposition of collagen, as revealed by Masson trichrome (Figure 9f). We were unable to detect pathology in extrapulmonary tissues of animals instilled with a sublethal dose of ricin, in contrast to the deposition of fibrin and glomerular leukocytosis that developed in kidneys in response to a lethal dose of

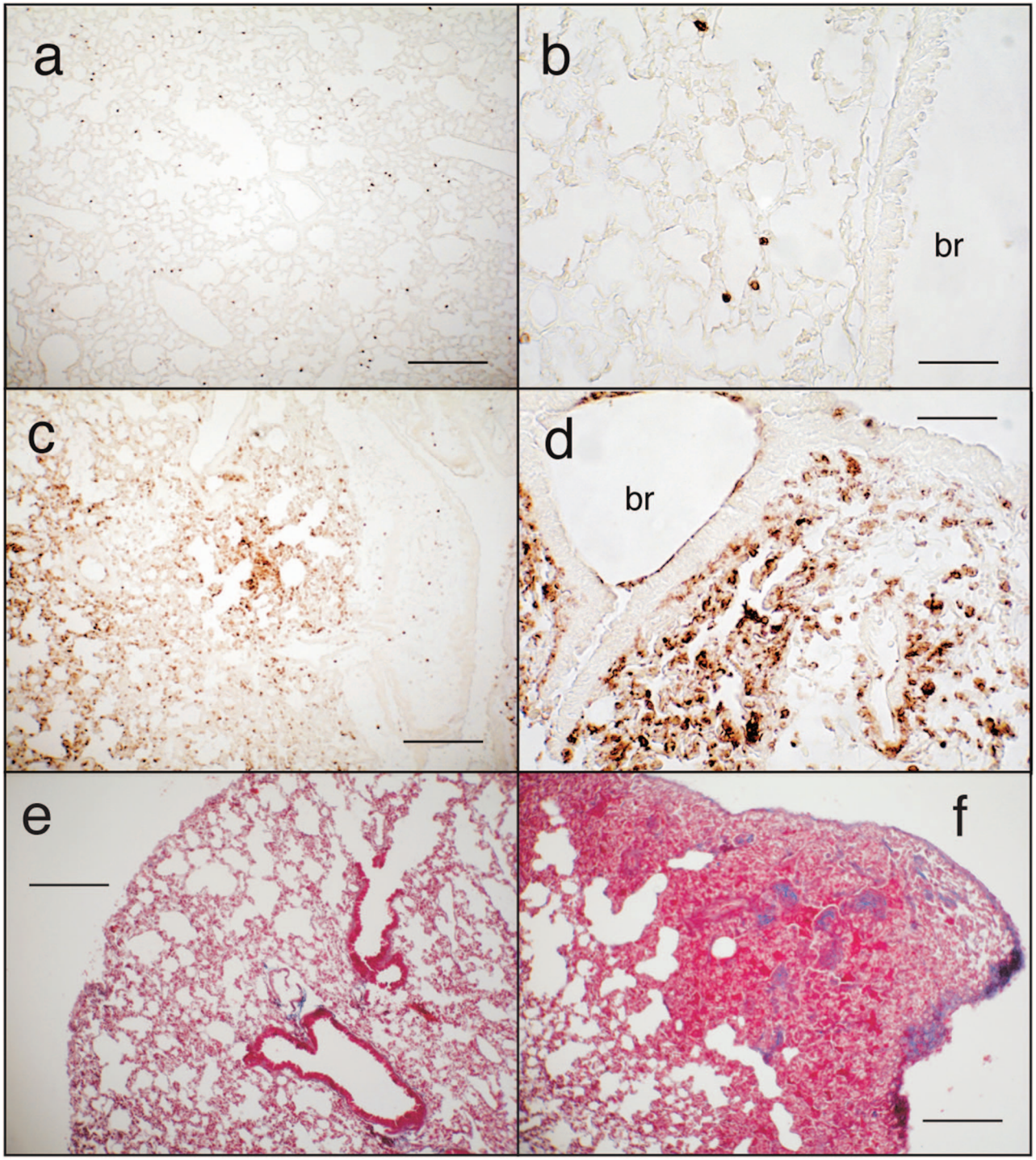

Figure 9. Immunohistochemical detection of Gr-1 (**a–d**) or collagen (Masson trichrome; **e**, **f**) after a sublethal dose of ricin. Mice were instilled with saline (**a**, **b**, and **e**) or 2 μg of ricin/100 g body weight (**c**, **d**, and **f**) and were sacrificed at 48 hours (**a–d**) or 4 weeks (**e** and **f**). br, bronchus. Scale bars: 200 μm (**a**, **c**, **e**, **f**); 50 μm (**b**, **d**). Original magnifications: ×100 (**a**, **c**, **e**, **f**); ×400 (**b**, **d**).

instilled ricin (Figure 7). Taken together, these data suggest that a sublethal dose of instilled ricin induced pathological responses in lungs that were similar to those induced by a lethal dose except for the presence of hemorrhage and deposition of fibrin. The pathological consequences of a sublethal dose of ricin appeared to be contained within the pulmonary tissues.

The disappearance of ricin-induced lesions in 28S rRNA may indicate the time interval required to fully resolve the ricin-induced damage. To approach this question, we determined the lifetime of ricin-induced lesions in 28S rRNA from lung after intratracheal administration of 2 μg of ricin/100 g body weight (Figure 6b). The results demonstrated that damage at A^{4256} became evident 6

hours after instillation of ricin and was maximal at 24 hours after treatment. Although by 7 days little change was detected in the abundance of lesions, by 14 days evidence of residual lesions was completely absent. These results suggested that either the damaged 28S rRNA was replaced by newly synthesized 28S rRNA in affected cells or that the cells containing damaged RNA had been eliminated from the lungs during the second week after administration.

In contrast to the appearance of substantial damage to 28S rRNA in a variety of extrapulmonary organs after a lethal dose of ricin (20 μg of ricin/100 g body weight; Figure 6a), administration of 2 μg of ricin/100 g body weight revealed an absence of detectable lesions in 28S rRNA from blood or liver (Figure 6b) and a weak, but detectable, band representing lesions in 28S rRNA from kidney and spleen (Figure 6b, asterisks). The confinement of 28S rRNA lesions primarily to the lungs of mice that received a sublethal dose of ricin suggests that this treatment did not lead to toxic levels of ricin within the systemic circulation.

We next determined whether mice responded to a nonlethal dose of ricin with increased expression of proinflammatory transcripts in lungs and in other organs. As shown in Figure 5 (filled bars), animals exposed to a nonlethal dose (2 μg of ricin/100 g body weight) induced levels of expression of proinflammatory transcripts in lungs that ranged from 30 to 100% of levels induced by the lethal dose. In contrast, expression of transcripts in extrapulmonary organs by the sublethal dose was in most cases significantly less than 10% of the levels induced by the lethal dose and in many cases was undetectable. An exception was IL-1β, expression of which in blood and spleen in response to a sublethal dose reached 40 to 50% of the levels induced by a lethal dose. These data suggest that, with the exception of IL-1β, the level of induced expression of proinflammatory mRNAs generally corresponded with the level of damage to 28S rRNA induced by instilled ricin.

Measurement of circulating cytokines and chemokines from animals instilled with a sublethal dose of ricin revealed increased levels of circulating TNF-α, IL-6, and CXCL1 (Figure 4b). Circulating levels of IL-1β and CCL2 in these animals were not elevated. We were unable to detect an increase in levels of blood urea nitrogen or creatinine (data not shown).

Discussion

Previous studies from our laboratory have shown that the depurination of 28S rRNA by ricin not only inhibited protein translation but also resulted in the activation of JNK and p38 MAPK by a pathway that is dependent on specific ribosomal damage and not on translational inhibition per se.[10,28,29] The activation of these kinases by inflammatory mediators is required for the increase in levels of mRNA that encode a large number of proinflammatory proteins, as shown by studies that have used small molecule inhibitors of JNK or p38 MAPK to suppress airway inflammation.[30] *In vitro* studies from our laboratory have demonstrated that concentrations of ricin that incompletely block protein synthesis not only induce expression of proinflammatory genes via the activation of JNK and p38 MAPK but also permits the productive translation of encoded proteins.[13] When injected into mice or rats, ricin induces the hallmarks of hemolytic uremic syndrome, which include increased plasma levels of inflammatory cytokines, deposition of fibrin/fibrinogen in renal glomeruli, and impaired kidney function.[13,16]

Our results demonstrate that instillation of either a lethal or sublethal dose of ricin resulted in severe injury and inflammation of airways and alveoli, characterized by influx of neutrophils, and apoptotic degeneration of macrophages and airway epithelium. In addition, the lethal dose of ricin produced focal areas of hemorrhage and necrosis. These data are consistent with previous reports on the histopathological effects of aerosolized ricin in animal systems.[20,21,31–33]

In addition, we have demonstrated that instilled ricin caused widespread nuclear localization of phosphorylated ERK, p38 MAPK, and JNK, but only phosphorylated p38 MAPK was evident in control lungs. These results are consistent with data obtained by immunoblotting, which demonstrated that ricin induced a large increase in phosphorylated JNK and ERK, but not p38 MAPK (Figure 3a). Ricin has been shown to lead to the activation of ERK1/2, JNK, and p38 MAPK in cultured cells[10,13,34] and in multiple organs in mice that have received ricin intravenously.[13] Using small molecule inhibitors in cultured macrophages to block ERK1/2, JNK, and p38 MAPK, singly and in combination, we previously demonstrated that the activation of proinflammatory genes by ricin requires the participation of these kinases. Taken together, these data support the conclusion that intratracheal delivery of ricin leads to the widespread activation of ERK1/2 and JNK in a variety of pulmonary cells. The elevated levels of phosphorylated p38 MAPK that are present in saline-instilled animals may be a consequence of the transient inflammation that is known to occur after instillation of saline.[35,36]

The MAPK family members are considered to be essential transducers of signals that lead to inflammatory responses.[11,37–40] DaSilva and colleagues[33] examined a limited number (n = 1176) of genes on cDNA arrays and found that 34 genes showed statistically significant changes in pulmonary gene expression after exposure of mice to inhaled ricin. Some of these transcripts were involved in tissue healing, regulation of inflammation, cell growth, apoptosis, and DNA repair. To obtain more comprehensive coverage of the mouse genome, we hybridized transcripts from lungs of control mice and ricin-instilled mice to the Affymetrix GeneChip Mouse Expression Set 430, which interrogates more than 39,000 transcripts (Supplementary Table 1, see *http://ajp.amjpathol.org*). In combination with EASE software, which automates biological theme analysis of annotated genes, we determined that transcripts involved in stress, immune, and inflammatory responses were the most frequently up-regulated and that the encoded molecules corresponded to cytokines, chemokines, and other ligands that bind to cell surface receptors (Table 1). Our

data from Affymetrix analysis was additionally verified for several induced transcripts by real-time RT-PCR (Figure 4). When compared with microarray analysis, real-time RT-PCR has greater sensitivity and accuracy and is able to produce quantitative data over a larger dynamic range. Comparison of transcript identities revealed that some chemokines and cytokines (eg, CCL20, CXCL1, CCL2, IL-23, IL-11, CXCL13, and CXCL16) were upregulated to a much greater extent after intratracheal than intravenous administration (Supplementary Table 1, see *http://ajp.amjpathol.org*), an outcome that would be expected if these transcripts originated within airway cells. We are currently pursuing studies in cultured airway cells to determine the set of genes that is uniquely activated in airway cells and to determine the potential role of those genes in ricin-mediated responses.

After instillation of a lethal dose of ricin, several extrapulmonary organs displayed increased levels of transcripts associated with inflammatory processes, although the increased expression was generally below the level of expression induced by ricin in lung tissue. Evidence for the direct action of ricin in extrapulmonary tissues was obtained by visualization of lesions in A^{4256} of 28S rRNA (Figure 6a) by applying a primer-extension assay developed in this laboratory.[10] Surprisingly, the measurement of damaged 28S rRNA molecules revealed that kidney and lung tissue contained approximately equal numbers of lesions in 28S rRNA after instillation of a lethal dose of ricin (Figure 6a). The high sensitivity of kidneys to circulating ricin may result from the large volume of cardiac output received by the kidneys (~20%) combined with the extensive network of microvasculature in these organs. In view of the evidence for direct action of ricin in kidneys, we investigated whether these organs could serve as a physiologically important target of instilled ricin. Intravenous administration of ricin resulted in deposition of fibrin/fibrinogen in renal glomeruli[13,16] and increased blood urea nitrogen and proteinuria,[13] suggesting that glomerular endothelium may represent a proximal target of ricin's actions. Development of impaired kidney function, as assessed by increased blood urea nitrogen and proteinuria, further implicated glomeruli as relevant targets of ricin.[13] As demonstrated in lung (Figure 2) and kidney (Figure 7, b and c) of the current study, instilled ricin led to the deposition of fibrin/fibrinogen in the microvasculature of these organs. The appearance of neutrophils in lung parenchyma (Figure 1) and renal glomeruli (Figure 7a), together with expression of E-selectin transcripts in lung (Figure 4) and kidney (Figure 5), suggests that ricin-mediated activation of endothelial cells is likely to be responsible for the recruitment of neutrophils into these tissues. In other experiments, we have determined that ricin induced the expression of proinflammatory transcripts in cultured endothelial cells (unpublished), consistent with the notion that direct action of ricin on the endothelium is responsible, at least in part, for the proteinuria (Figure 8) and increased blood urea nitrogen that occurred after instillation of ricin.

In contrast to effects of a lethal dose of ricin, animals receiving a sublethal dose of ricin showed little or no evidence of systemic dissemination of the toxin. The histopathology and increased expression of inflammatory genes in pulmonary tissues in animals receiving both lethal and sublethal amounts of ricin were quite similar, as were the levels of damage to 28S rRNA. However, only the lethal dose resulted in regions of focal hemorrhage. We suggest that the associated hemorrhage caused by the higher dose of ricin may be responsible for causing the entrance of ricin into the systemic circulation, either directly into the vasculature or indirectly through lymphatic drainage.

Exposure of mice to a sublethal dose of ricin permitted us to examine residual effects of ricin on pulmonary tissues after resolution of the inflammatory response. Several weeks after recovery from the acute effects of ricin, lungs displayed areas of collagen deposition in which there occurred total obliteration of alveolar architecture. Relevant to potential exposure of human populations to ricin, it is apparent that individuals who have been exposed to aerosolized ricin should receive continuing management for acute lung injury.

The increased appearance of circulating proinflammatory mediators after instillation of a lethal dose of ricin may result exclusively from synthesis within pulmonary tissues or, alternatively, from the direct action of circulating ricin on other organs. Although CCL2 was elevated exclusively in sera from animals exposed to a lethal dose of ricin (Figure 4), other cytokines (TNF-α, IL-6, and CXCL1) were elevated to similar levels in animals receiving either a lethal or sublethal dose (Figure 4). The presence of elevated levels of TNF-α, IL-6, and CXCL1 in sera of mice in the absence of apparent renal pathology suggests that impairment of kidney function by exposure to a lethal dose of ricin resulted primarily from the direct action of ricin on 28S rRNA in these organs rather than from the effects of circulating mediators. Nevertheless, the presence of circulating inflammatory mediators may contribute to the inflammatory state that develops in extrapulmonary tissues in response to the direct action of ricin.

The results of these studies demonstrate that introduction of ricin through the pulmonary system may achieve systemic distribution that could lead to impaired function of kidneys and perhaps other organs. These studies suggest that health care personnel should be cognizant of the potential systemic inflammatory responses in the event that human populations would be exposed to aerosolized ricin and that kidney function should be closely monitored to provide necessary supportive care. The presence of residual lung pathology after a sublethal dose of intratracheal ricin suggests that human populations exposed to ricin should be monitored well after resolution of initial injury and may need continuing supportive therapy. In addition, we propose that the identification of lesions in 28S rRNA in patient blood or cells of bronchoalveolar lavage fluid may indicate the extent of toxic damage to inhaled ricin. Close monitoring of circulating cytokines and chemokines in these patients may facilitate assessment of the severity of toxicity and the course of recovery.

Investigators that have administered ricin to animals by aerosolization have concluded that the pathological effects of ricin are confined exclusively to pulmonary tis-

sues.[19–21,31,41] Although the experimental introduction of ricin by aerosolization closely replicates the anticipated mode of delivery to human populations, introduction of the toxin by instillation has several advantages, as discussed in a recent review that enumerates the uses and limitations of instillation.[35] The advantages of instillation include: 1) the ability to deliver a range of well-defined doses within a short time to large numbers of animals; 2) the avoidance of exposure of nonpulmonary tissues, which could result in substantial quantities of ricin entering the gastrointestinal tract during exposure and during subsequent preening; 3) the ability to perform multiple experiments in animals when the amount of material for study is limited; and, importantly, 4) minimization of risks to laboratory workers. However, it should be appreciated that the effective dose rates of instilled toxins are substantially greater than that which would be achieved during inhalation. For example, the LD_{50} of instilled ricin in C57BL6 mice in our studies was 10 μg/100 g body weight, compared with aerosolized ricin in BALB/c mice of 1.4 μg/100 g body weight.[33] In addition, the intrapulmonary distribution of instilled liquids occurs nonuniformly and favors the upper portions of the respiratory tract. As a result of focally high lung burdens that occur after instillation, adverse pulmonary responses may be exaggerated when compared with delivery by aerosolization.

Although outcomes may differ when ricin is administered by instillation versus aerosolization, our results nevertheless suggest the possibility that ricin may be disseminated outside the pulmonary system and may lead to renal failure and perhaps other organ-specific pathologies. The entrance of ricin into the systemic circulation of human victims after exposure to aerosolized ricin may occur should individuals be exposed to high concentrations for extended times and/or within confined spaces close to the source of the released toxin. Increased understanding of the inflammatory ligands, their receptors, and the signaling pathways that participate in the local and disseminated inflammatory responses may lead to development of therapeutic modalities that would reduce or eliminate many of the consequences of ricin toxicity.

Acknowledgment

We thank Olga Ryabinina for important technical contributions.

References

1. Cookson J, Nottingham J: A Survey of Chemical and Biological Warfare. New York, Monthly Review Press, 1969, p 6
2. Crompton R, Gall D: Death in a pellet. Med Leg J 1980, 48:51–62
3. Kifner J: Man is arrested in a case involving deadly poison. New York Times, 1995 Dec 23, p A-7
4. Shar L: Probe aims at sale of deadly bacteria. USA Today, 1995 July 11, p 2-A
5. Goodman PS: Seized poison set off few alarms. Anchorage Daily News, 1996 Jan 4, p B-1
6. Mayor N: UK doctors warned after ricin poison found in police raid. Br Med J 2003, 326:126
7. Sandvig K, Grimmer S, Lauvrak SU, Torgersen ML, Skretting G, van Deurs B, Iversen TG: Pathways followed by ricin and Shiga toxin into cells. Histochem Cell Biol 2002, 117:131–141
8. Olsnes S, Kozlov JV: Ricin. Toxicon 2001, 39:1723–1728
9. Montanaro L, Sperti S, Mattioli A, Testoni G, Stirpe F: Inhibition by ricin of protein synthesis in vitro. Inhibition of the binding of elongation factor 2 and of adenosine diphosphate-ribosylated elongation factor 2 to ribosomes. Biochem J 1975, 146:127–131
10. Iordanov MS, Pribnow D, Magun JL, Dinh TH, Pearson JA, Chen SL, Magun BE: Ribotoxic stress response: activation of the stress-activated protein kinase JNK1 by inhibitors of the peptidyl transferase reaction and by sequence-specific RNA damage to the alpha-sarcin/ricin loop in the 28S rRNA. Mol Cell Biol 1997, 17:3373–3381
11. Karin M, Gallagher E: From JNK to pay dirt: Jun kinases, their biochemistry, physiology and clinical importance. IUBMB Life 2005, 57:283–295
12. Saklatvala J, Dean J, Clark A: Control of the expression of inflammatory response genes. Biochem Soc Symp 2003, (70):95–106
13. Korcheva V, Wong J, Corless C, Iordanov M, Magun B: Administration of ricin induces a severe inflammatory response via nonredundant stimulation of ERK, JNK, and P38 MAPK and provides a mouse model of hemolytic uremic syndrome. Am J Pathol 2005, 166:323–339
14. Stirpe F, Battelli MG: Ribosome-inactivating proteins: progress and problems. Cell Mol Life Sci 2006, 63:1850–1866
15. Proulx F, Seidman EG, Karpman D: Pathogenesis of Shiga toxin-associated hemolytic uremic syndrome. Pediatr Res 2001, 50:163–171
16. Taylor CM, Williams JM, Lote CJ, Howie AJ, Thewles A, Wood JA, Milford DV, Raafat F, Chant I, Rose PE: A laboratory model of toxin-induced hemolytic uremic syndrome. Kidney Int 1999, 55:1367–1374
17. Williams JM, Lote CJ, Thewles A, Wood JA, Howie AJ, Williams MC, Adu DA, Taylor CM: Role of nitric oxide in a toxin-induced model of haemolytic uraemic syndrome. Pediatr Nephrol 2000, 14:1066–1070
18. Franz DR, Jaax JK: Ricin toxin. Textbook of Military Medicine, part 1. Warfare, Weaponry, and the Casualty: Medical Aspects of Chemical and Biological Warfare. Edited by FR Sidell, ET Takfuji, DR Franz. Washington, Office of the Surgeon General, Department of the Army, 1997, pp 631–642
19. Brown RF, White DE: Ultrastructure of rat lung following inhalation of ricin aerosol. Int J Exp Pathol 1997, 78:267–276
20. Griffiths GD, Rice P, Allenby AC, Bailey SC, Upshall DG: Inhalation toxicology and histopathology of ricin and abrin toxins. Inhal Toxicol 1995, 7:269–288
21. Doebler JA, Wiltshire ND, Mayer TW, Estep JE, Moeller RB, Traub RK, Broomfield CA, Calamaio CA, Thompson WL, Pitt ML: The distribution of [125I]ricin in mice following aerosol inhalation exposure. Toxicology 1995, 98:137–149
22. Vestweber D, Blanks JE: Mechanisms that regulate the function of the selectins and their ligands. Physiol Rev 1999, 79:181–213
23. Senftleben U, Karin M: The IKK/NF-kappa B pathway. Crit Care Med 2002, 30:S18–S26
24. Kyriakis JM, Avruch J: Mammalian mitogen-activated protein kinase signal transduction pathways activated by stress and inflammation. Physiol Rev 2001, 81:807–869
25. Bonizzi G, Karin M: The two NF-kappaB activation pathways and their role in innate and adaptive immunity. Trends Immunol 2004, 25:280–288
26. Hosack DA, Dennis Jr G, Sherman BT, Lane HC, Lempicki RA: Identifying biological themes within lists of genes with EASE. Genome Biol 2003, 4:R70
27. Hestdal K, Ruscetti FW, Ihle JN, Jacobsen SE, Dubois CM, Kopp WC, Longo DL, Keller JR: Characterization and regulation of RB6–8C5 antigen expression on murine bone marrow cells. J Immunol 1991, 147:22–28
28. Iordanov MS, Magun BE: Different mechanisms of c-Jun NH(2)-terminal kinase-1 (JNK1) activation by ultraviolet-B radiation and by oxidative stressors. J Biol Chem 1999, 274:25801–25806
29. Iordanov MS, Choi RJ, Ryabinina OP, Dinh TH, Bright RK, Magun BE: The UV (ribotoxic) stress response of human keratinocytes involves the unexpected uncoupling of the Ras-extracellular signal-regulated kinase signaling cascade from the activated epidermal growth factor receptor. Mol Cell Biol 2002, 22:5380–5394
30. Adcock IM, Chung KF, Caramori G, Ito K: Kinase inhibitors and airway inflammation. Eur J Pharmacol 2006, 533:118–132

31. Wilhelmsen CL, Pitt ML: Lesions of acute inhaled lethal ricin intoxication in rhesus monkeys. Vet Pathol 1996, 33:296–302
32. Poli MA, Rivera VR, Pitt ML, Vogel P: Aerosolized specific antibody protects mice from lung injury associated with aerosolized ricin exposure. Toxicon 1996, 34:1037–1044
33. DaSilva L, Cote D, Roy C, Martinez M, Duniho S, Pitt ML, Downey T, Dertzbaugh M: Pulmonary gene expression profiling of inhaled ricin. Toxicon 2003, 41:813–822
34. Iordanov MS, Pribnow D, Magun JL, Dinh TH, Pearson JA, Magun BE: Ultraviolet radiation triggers the ribotoxic stress response in mammalian cells. J Biol Chem 1998, 273:15794–15803
35. Driscoll KE, Costa DL, Hatch G, Henderson R, Oberdorster G, Salem H, Schlesinger RB: Intratracheal instillation as an exposure technique for the evaluation of respiratory tract toxicity: uses and limitations. Toxicol Sci 2000, 55:24–35
36. Shami SG, Thibodeau LA, Kennedy AR, Little JB: Proliferative and morphological changes in the pulmonary epithelium of the Syrian golden hamster during carcinogenesis initiated by 210Po alpha alpha-radiation. Cancer Res 1982, 42:1405–1411
37. Duan W, Chan JH, Wong CH, Leung BP, Wong WS: Anti-inflammatory effects of mitogen-activated protein kinase kinase inhibitor U0126 in an asthma mouse model. J Immunol 2004, 172:7053–7059
38. Jaffee BD, Manos EJ, Collins RJ, Czerniak PM, Favata MF, Magolda RL, Scherle PA, Trzaskos JM: Inhibition of MAP kinase kinase (MEK) results in an anti-inflammatory response in vivo. Biochem Biophys Res Commun 2000, 268:647–651
39. Arndt PG, Young SK, Lieber JG, Fessler MB, Nick JA, Worthen GS: Inhibition of c-Jun N-terminal kinase limits lipopolysaccharide-induced pulmonary neutrophil influx. Am J Respir Crit Care Med 2005, 171:978–986
40. Lee JC, Kumar S, Griswold DE, Underwood DC, Votta BJ, Adams JL: Inhibition of p38 MAP kinase as a therapeutic strategy. Immunopharmacology 2000, 47:185–201
41. Griffiths GD, Allenby AC, Bailey SC, Hambrook JL, Rice P, Upshall DG: The Inhalation Toxicity of Ricin Purified "In-House" from the Seeds of Ricinus Communis Var, Zanzibariensis. Salisbury, Ministry of Defense, Porton Down, 1994